Inorg. Chem. **2008**, *47*, 5775−5779

Structures of $[(n\text{-}C_4H_9)_2NH_2]_2Cd_9Cl_{20}\cdot 2H_2O$ and $[Cu(C_{14}H_{24}N_4)]_2Cu_{13}Cl_{30}(H_2O)_2\cdot xH_2O$: Perforated Layer Structures Based on the $CdCl_2$ Layer Network

Adrienne A. Thorn and Roger D. Willett*

Department of Chemistry, Washington State University, Pullman, Washington 99163

Brendan Twamley

University Research Office, University of Idaho, Moscow, Idaho 88343

Received January 16, 2008

The crystal structures are reported for two compounds containing novel perforated layer structures, $[DBA]_2Cd_9Cl_{20}\cdot 2H_2O$ and $[Cu(TIM)]_2Cu_{13}Cl_{30}(H_2O)_2\cdot xH_2O$, where $[DBA]^+$ = di*n*-butylammonium and TIM = 2,3,9,10-tetramethyl-1,3,8,10-tetraenecyclo- 1,4,8,11-tetraazatetradecane. In the former compound, single Cd^{2+} ions are excised from the parent $CdCl_2$ layers, with water molecules hydrogen bonded to chloride ions on both sides of the excision. Lattice stability is provided by the DBA^+ cations, which have an all-trans conformation. These lie between the layers, hydrogen bonding to the adjacent $[Cd_9Cl_{20}(H_2O)_2]_n^{2n-}$ sheets. In the copper compound, the modification of the parent $CuCl_2$ structure is much more complex. In this compound, $[Cu_2Cl_2]^{2+}$ moieties are excised in a regular fashion. In addition, at 50% of the Cu1 sites, $CuCl_2$ species are replaced by pairs of water molecules in a random fashion. The $Cu(TIM)^{2+}$ cations bridge the layers via the formation of two semicoordinate bonds to chloride ions at the edge of the $[Cu_2Cl_2]^{2+}$ excision sites of adjacent layers.

Introduction

The synthesis and characterization of novel low-dimensional organoammonium metal halide salts has been an area of major emphasis in our laboratory. While much of the effort has focused on copper(II) halide salts,[1] studies of systems involving other metal ions have also been investigated.[2] Because of both the variability of the metal ion coordination geometry and of the bridging capabilities of the halide ions, as well as the geometrical constraints associated with the organoammonium ions, the a priori prediction of crystal structures has been problematic. Hence, the use of traditional design tools has had limited success. Instead, we have used a "retro-crystal engineering" descriptive approach to better understand more complex structures and to develop a methodology for systematic structure design.[3] Many low dimensional networks can be described as segments of higher-dimensional metal halide frameworks, and thus the analysis method referred to as "dimensional reduction" has been coined.[3d,g,4] Tulsky and Long have previously applied this idea to a wide variety of inorganic salts using parent lattices from binary MX_n structures.[5]

* To whom correspondence should be addressed. E-mail: rdw@mail.wsu.edu.

(1) For example, see: (a) Geiser, U.; Gaura, R. M.; Willett, R. D.; West, D. X. *Inorg. Chem.* **1986**, *25*, 4203. (b) O'Brien, S.; Gaura, R. M.; Landee, C. P.; Ramakrishna, B. L.; Willett, R. D. *Inorg. Chim. Acta* **1987**, *141*, 83. (c) Willett, R. D. *Acta Crystallogr.* **1988**, *B44*, 503. (d) Willett, R. D.; Place, H.; Middleton, M. *J. Am. Chem. Soc.* **1988**, *110*, 8639. (e) Patyal, B. R.; Willett, R. D. *Magn. Res. Rev.* **1990**, *15*, 47. (f) Halvorson, K.; Patterson, C.; Willett, R. D. *Acta Crystallogr.* **1990**, *B46*, 508. (g) Willett, R. D.; Bond, M. R.; Pon, G. *Inorg. Chem.* **1990**, *29*, 4160. (h) Willett, R. D.; Awwadi, F.; Butcher, R.; Haddad, S.; Twamley, B. *Cryst. Growth Des.* **2003**, *3*, 301.

(2) (a) Pressprich, M. R.; Bond, M. R.; Willett, R. D.; Zuniga, F. J.; Cabezudo, M. J. *Acta Crystallogr.* **1991**, *B47*, 337. (b) Bond, M.; Willett, R. D. *Acta Crystallogr.* **1993**, *C49*, 861. (c) Pressprich, M. R.; Bond, M. R.; Willett, R. D. *J. Phys. Chem. Solids* **2002**, *63*, 79. (d) Willett, R. D.; Maxcy, K. R.; Twamley, B. *Inorg. Chem.,* **2002**, *41*, 7024. (e) Maxcy, K. R.; Willett, R. D.; Mitzi, D. *Acta Crystallogr.* **2003**, *E59*, m364.

(3) (a) Desiraju, G. R. *J. Mol. Struct.* **2003**, *656*, 5. (b) Desiraju, G. R. *J. Indian Chem. Soc.* **2003**, *80*, 151. (c) Desiraju, G. R. *Chem. Commun.* **1997**, 1475. (d) Haddad, S.; Awwadi, F.; Willett, R. D. *Cryst. Growth Des.* **2003**, *3*, 501. (e) Nangia, A.; Desiraju, G. R. *NATO Sci. Series C* **1999**, *519*, 193. (f) Thalladi, V. R.; Goud, B. S.; Hoy, V. J.; Allen, F. H.; Howard, J. A.; Desiraju, G. R. *Chem. Commun.* **1996**, 401. (g) Thorn, A.; Willett, R. D.; Twamley, B. *Cryst. Growth Des.* **2005**, *5*, 673.

10.1021/ic8000834 CCC: $40.75
Published on Web 05/28/2008

We have generalized the Tulsky and Long approach to include lattice networks derived from the following three parent structure types: the cubic AMX_3 perovskite structure containing a three-dimensional array of corner-shared octahedra,[6] the hexagonal MX_2 structure that contains edge-shared octahedral layers,[7] and the hexagonal AMX_3 structure which has chains of face-shared octahedra.[8] In the dimensional reduction concept, the organic cationic species, typically protonated amines, can be conceptualized as "molecular scissors" to sever the M−X−M bridges of the parent lattice. The use of monoalkylammonium cations typically leads to the formation of $(RNH_3)_2MX_4$ layer perovskite networks. These have proved useful in the study of two-dimensional magnetism[9] and in the design of hybrid semiconducting materials.[10] The tribridged AMX_3 structures are typically found when the organic cation has little or no hydrogen bonding capabilities.[11] With halometallate compounds that contain edge-shared octahedra, the extended structures observed are typically composed of $(M_nX_{2n+2})_m^{2m+}$ ribbons in which these species retain the edge-shared octahedra concatenation motif.[12] Unfortunately, no systematic synthetic approach has been developed to predict these structures.

In a few cases, however, perforated layer structures have been obtained in which small $(M_nX_{2n-2})^{2+}$ fragments have been systematically excised from the edge-shared MX_2 layers. The known examples have been obtained with PnR_4^+ cations, such as $P(CH_3)_4^+$ or $CH_3N(C_2H_5)_3^+$, that have no hydrogen bonding capabilities.[13] Thus, the perforation of the layers has been driven by simple electrostatic forces. In this paper, we report the crystal structures of two compounds containing novel perforated layer structures, $[DBA]_2[Cd_9Cl_{20}]\cdot 2H_2O$ and $[Cu(TIM)]_2Cu_{13}Cl_{30}(H_2O)_2\cdot xH_2O$, where DBA^+ = di-*n*-butylammonium and TIM = 2,3,9,10-tetramethyl-1,3,8,10-tetraenecyclo-1,4,8,11-tetraazatetradecane. These two structures present new modes of interaction that lead to perforation of the MX_2 layers. In the former, the DBA^+ cations hydrogen bond to water molecules that, in turn, hydrogen bond to the layers where single Cd^{2+} ions have been excised. In the latter, the $Cu(TIM)^{2+}$ cations bridge between adjacent layers by forming semicoordinate Cu···Cl bonds to chloride ions in the layers. This leads to the systematic excision of $(Cu_2Cl_2)^{2+}$ fragments and, in addition, the random excision of neutral $CuCl_2$ units with the concomitant insertion of pairs of water molecules.

Experimental Section

Crystals of $[DBA]_2[Cd_9Cl_{20}]\cdot 2H_2O$ were prepared by dissolution of [DBA]Cl (0.181 g, 1 mmol) and $CdCl_2$ (0.601 g, 3 mmol) in a solution of methanol (10 mL), nitromethane (10 mL), and water (2 mL). Most of the solvent was evaporated by gentle heating, and the clear, colorless solution was then allowed to crystallize slowly at room temperature. Bis(dibutylammonium) icosachlorononacadmate(II) dihydrate crystals formed after four days as thin clear, colorless, flat parallelepipeds. Crystals were removed from solution and immediately placed in hydrocarbon oil to prevent solvent loss from the crystalline material.

The compound $[Cu(TIM)]_2Cu_{13}Cl_{30}(H_2O)_2\cdot xH_2O$ was prepared as follows:[14] A 10-mL beaker with an acetonitrile solution of 0.34 g of $CuCl\cdot 2H_2O$ (2.0 mmol) and 1.43 g of Bu_4NCl (4.0 mmol) was placed in a 50 mL beaker. A 0.62 g (1.0 mmol, $x = 1$) amount of solid $Cu(TIM)_xH_2O(PF_6)$ was placed in the bottom of the 50 mL beaker, and acetonitrile was then carefully added to the 50 mL beaker until the lip of the smaller beaker was covered with approximately 0.5 cm of the solvent. At this point, the mouth of the outer 50 mL beaker was covered with parafilm, and the nested beakers were allowed to sit at room temperature as dissolution of the $Cu(TIM)\cdot xH_2O(PF_6)$ and diffusion of the solutions took place. Over the course of several days, black prismatic crystals formed. The crystals were collected by filtration, washed with a small amount (about 2 mL) of acetonitrile, and air-dried.

For each compound, a suitable crystal was selected, attached to a glass fiber and placed immediately in the low-temperature nitrogen stream.[15] Data was collected at ~86(2) K using a Bruker/Siemens SMART APEX instrument (Mo Kα radiation, $\lambda = 0.71073$ Å) equipped with a Cryocool NeverIce low-temperature device. Data was measured using ω scans of 0.3° per frame with different exposures (see Table 1), and a full sphere of data was collected in each case. Cell parameters were retrieved using SMART[16] software

(4) (a) Axtell, E.A.(III).; Liao, J. H.; Pikramenou, Z.; Kanatzidis, M. G. *Chem.—Eur. J.* **1996**, *2*, 656. (b) Bietenholz, W.; Gfeller, A.; Wiese, U. J. *J. High Energy Phys. (online)* **2003**. (c) Gatta, G. D.; Masci, S.; Vivani, R. *J. Mater. Chem.* **2003**, *13*, 1215. (d) Long, J. R.; McCarty, L. S.; Holm, R. H. *J. Am. Chem. Soc.* **1996**, *118*, 4603. (e) Long, J. R.; Williamson, A. S.; Holm, R. H. *Angew. Chem., Int. Ed.* **1995**, *34*, 226. (f) Tulsky, E. G., Ph.D. Thesis, University of California, Berkeley, CA, 2002. (g) Tulsky, E. G.; Long, J. R. *Inorg. Chem.* **2001**, *40*, 6990.

(5) Tulsky, E. G.; Long, J. R. *Chem. Mater.* **2001**, *13*, 1149.

(6) Siegel, S.; Gebert, E. *Acta Crystallogr.* **1964**, *17*, 790.

(7) Pauling, L.; Hoard, J. L. *Z. Kristallogr. Kristallgeom. Kristallphys. Kristallchem.* **1930**, *74*, 546.

(8) Smirvona, L.; Brager, A.; Zhdanov, H. *Acta Physicochim.* **1941**, *15*, 255.

(9) (a) Willett, R. D.; Place, H.; Middleton, M. *J. Am. Chem. Soc.* **1988**, *110*, 8639. (b) Willett, R. D.; Jardine, F. H.; Rouse, I.; Wong, R. J. H.; Landee, C. P. *Phys. Rev.* **1981**, *B24*, 5372. (c) Zhou, P.; Drumheller, J. E.; Patyal, B.; Willett, R. D. *Phys. Rev. B* **1992**, *45*, l2365.

(10) (a) Koutselas, I. B.; Mitzi, D. B.; Papavassiliou, G. C.; Papaioannou, G. J.; Krautscheid, H. *Synth. Met.* **1997**, *86*, 2171. (b) Mitzi, D. B. *Chem. Mater.* **1996**, *8*, 791. (c) Mitzi, D. B.; Dimitrakopoulos, C. D.; Kosbar, L. L. *Chem. Mater.* **2001**, *13*, 3728. (d) Mitzi, D. B.; Kagan, C. R. *Thin-Film Transistors* **2003**, 457. (e) Mitzi, D. B.; Wang, S.; Field, C. A.; Chess, C. A.; Guloy, A. M. *Science* **1995**, *267*, 1473. (f) O'Brien, S.; Guara, R. M.; Landee, C. P.; Willett, R. D. *Solid State Commun.* **1981**, *39*, 1333. (g) Xu, Z.; Mitzi, D. B. *Inorg. Chem.* **2003**, *42*, 6589. (h) Xu, Z.; Mitzi, D. B.; Dimitrakopoulos, C. D.; Maxcy, K. R. *Inorg. Chem.* **2003**, *42*, 2031. (i) Mitzi, D. B. *Chem. Mater.* **2001**, *13*, 3283. (j) Mitzi, D. B. *J. Chem. Soc., Dalton Trans.* **2001**, (k) Mitzi, D. B.; Field, C. A.; Harrison, W. T. A.; Guloy, A. M. *Nature* **1994**, *369*, 467. (l) Yamada, T.; Kobatake, S.; Muto, K.; Irie, M. *J. Am. Chem. Soc.* **2000**, *122*, 1589.

(11) For example, see: (a) Krishnam, V. G.; Dou, S-q.; Weiss, A. *Z. Naturforsch., A* **1991**, *46*, 1063. (b) Morosin, B. *Acta Crystallogr., Sect.B* **1972**, *28*, 2303. (c) Hassen, R. B.; Salah, A. B.; Kallel, A.;; Daoud, A.; Jaud, J. *J. Chem. Cryst.* **2002**, *32*, 427. (d) Asahum, R.; Hasebe, K.; Gesi, K. *Acta Crystallogr., Sect.B* **1991**, *47*, 1208.

(12) (a) Thorn, A.; Willett, R. D.; Twamley, B. *Cryst. Growth Des.* **2006**, *6*, 1134. (b) Willett, R. D.; Bond, M. R.; Pon, G. *Inorg. Chem.* **1990**, *29*, 4160. (c) Bond, M. R.; Willett, R. D. *Inorg. Chem.* **1989**, *38*, 3267. (d) Willett, R. D.; Maxcy, K. R.; Twamley, B. *Inorg. Chem.* **2002**, *41*, 7024.

(13) (a) Weise, S.; Willett, R. D. *Acta Crystallogr., Sect C* **1993**, *49*, 283. (b) Haije, W. G.; Dobbelaar, J. A. L.; Maaskant, W. J. A. *Acta Crystallogr., Sect C* **1986**, *42*, 1485. (c) Murray, K.; Willett, R. D. *Acta Crystallogr., Sect C* **1993**, *49*, 1739. (d) Santos, I. C.; Henriques, R. T.; Almeida, M.; Alcácer, L.; Duarte, M. T. *Inorg. Chem.* **1996**, *35*, 168.

(14) Vasilevesky, I. Ph.D. thesis, University of Washington, Seattle, WA, 1988.

(15) Hope, H. *Prog. Inorg. Chem.* **1994**, *41*, 1.

(16) *SMART*, version 5.626; Bruker AXS: Madison, WI, 2002.

Table 1. Summary of Data Collection and Refinement Parameters

	$[DBA]_2[Cd_9Cl_{20}]\cdot 2H_2O$	$[Cu(TIM)]_2Cu_{13}Cl_{30}(H_2O)_2\cdot xH_2O$
empirical formula	$C_{16}H_{44}Cd_9Cl_{20}N_2O_2$	$C_{14}H_{25.40}Cl_{15}Cu_{7.51}N_4O_{1.28}$
fw	2017.13	1279.20
temp (K)	86(2)	89(2)
description	colorless parallelepiped	orange plate
size (mm^3)	0.23 × 0.06 × 0.05	0.17 × 0.17 × 0.10
syst	triclinic	triclinic
space group	$P\bar{1}$	$P\bar{1}$
Z	1	1
a (Å)	9.9812(11)	9.4539(13)
b (Å)	10.1132(11)	9.7873(13)
c (Å)	13.3633(15)	10.9255(15)
α (deg)	71.150(2)	98.7616(10)
β (deg)	86.149(2)	107.115(2)
γ (deg)	86.137(2)	109.192(2)
V ($Å^3$)	1272.2(2)	877.0(2)
exposure (s)	5	20
D_{calcd} (Mg m^{-3})	2.633	2.422
reflns used	4599	3178
GOF	0.867	1.060
R[a] indices [$I > 2\sigma(I)$]	R1 = 0.0417	R1 = 0.0228
	wR2 = 0.0888	wR2 = 0.0602
R[a] indices (all data)	R1 = 0.0666	R1 = 0.0247
	wR2 = 0.1003	wR2 = 0.0614

[a] $R1 = \sum||F_o| - |F_c||/\sum|F_o|$; $wR2 = \{\sum[w(F_o^2 - F_c^2)^2]/ \sum[w(F_o^2)^2]\}^{1/2}$.

and refined using SAINTPlus[17] on all observed reflections. Data reduction and correction for Lp and decay were performed using the SAINTPlus[17] software. Absorption corrections were applied using SADABS.[18] The structures were solved by direct methods and refined by the least-squares method on F^2 using the SHELXTL program package.[19] The structure of $[DBA]_2[Cd_9Cl_{20}]\cdot 2H_2O$ was solved in the space group $P\bar{1}$. Water molecule hydrogen atoms were placed in calculated positions and all non-hydrogen atoms were refined anisotropically. The structure of $[Cu(TIM)]_2Cu_{13}Cl_{30}(H_2O)_2\cdot xH_2O$ was also solved in the space group $P\bar{1}$. Several of the atoms were observed to be disordered or present with partial occupancy. Various models for the refinement of these atoms always yielded results with occupancy factors close to 0.5 for Cu1, Cl8, and O8 and ~0.14 for O2 (the lattice−water molecule). In the final refinement, Cu1, Cl8, and O8 were modeled as 50% occupancy, and the occupancy factor for O2 refined to a value of 0.14. O2 was held isotropic, and all other non-hydrogen atoms were refined anisotropically. No decomposition was observed during data collection for either crystal.

Structure Descriptions

$[DBA]_2[Cd_9Cl_{20}]\cdot 2H_2O$. This structure illustrates the simplest modification of the layered hexagonal MX_2 type structures. The reaction of an organoammonium cation with cadmium chloride creates perforated layers of the $CdCl_2$ parent structure, whereby single Cd atoms have been excised. Figure 1 shows the asymmetric unit of this compound, augmented to illustrate the octahedral coordination of all five crystallographically independent cadmium atoms. Also present in this structure are $[DBA]^+$ cations and water molecules. Both play an important role in the stabilization of the unique layer formation in this compound through hydrogen bonding. The perforated $CdCl_2$ sheets lie parallel to the [1 0 0] plane of the unit cell. The removal of single cadmium atoms from

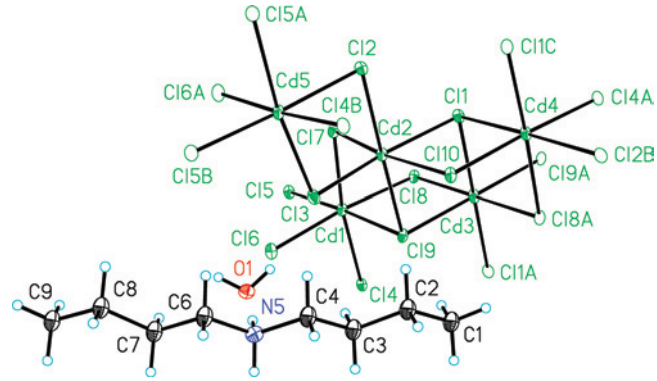

Figure 1. Illustration of the asymmetric unit of the $[DBA]_2[Cd_9Cl_{20}]\cdot 2H_2O$ structure. The octahedral coordination of each cadmium(II) atom has been completed with symmetry-related atoms (open ellipsoids). Thermal ellipsoids are shown at the 50% probability level.

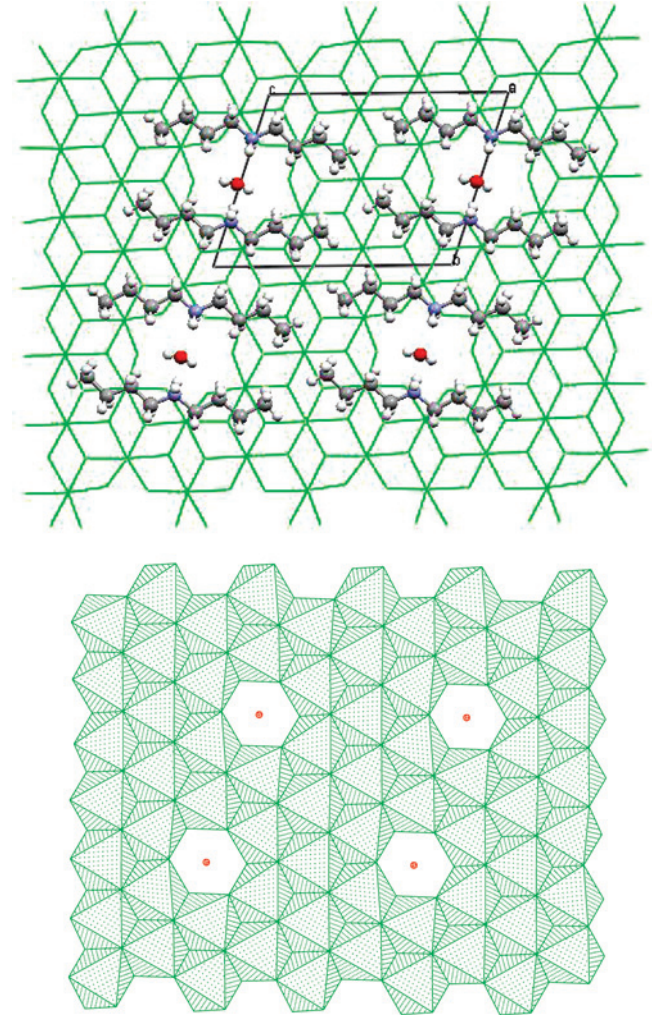

Figure 2. Ball and stick (top) and polyhedral (bottom) representation of a single $[DBA]_2[Cd_9Cl_{20}]\cdot 2H_2O$ layer lying in the *bc* plane (with the *c*-axis oriented horizontally in the figure). The top diagram shows the water molecules and $[DBA]^+$ cations that lie above each layer, while the bottom diagram only shows the oxygen atoms (red balls) of the water molecules that cap the octahedral holes.

these sheets creates the octahedral cavities shown in Figure 2. Significant distortions in the Cd−Cl bond lengths are observed near the octahedral cavities, with the Cd−Cl distances ranging from 2.538(2) to 2.687(2) Å and *cis*-Cl−Cd−Cl angles ranging between 84.48(6) and 98.71(6)°,

(17) *SAINTPlus*, version 6.36a; Bruker AXS: Madison, WI, 2001.
(18) *SADABS*, version 2.01; Bruker AXS, Inc.: Madison, WI, 2001.
(19) Sheldrick, G. M. *SHELXTL*, version 6.10; , Bruker AXS Inc.: Madison, WI, 2001.

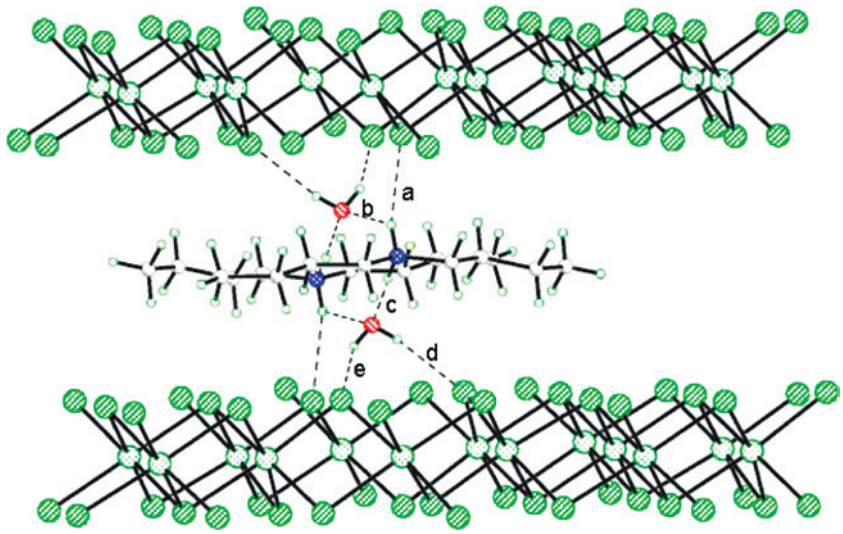

Figure 3. Illustration of the hydrogen bonding (dashed lines) between the $[DBA]^+$ cations, water molecules, and $CdCl_2$ sheets via N−H···O, N−H···Cl, and O−H···Cl contacts. Hydrogen bond distances and angles: D−A (Å), D−H···A (deg), (a) N1−H1E···Cl6# = 3.314, 155.6; (b) N1−H1E···O1# = 2.958, 121.6; (c) N1−H1D···O1 = 2.784, 177.2; (d) O1−H··Cl7$ = 3.147, 165.9; (e) O1−H1···Cl3 = 3.132, 149.5. Transformations: # = 3 − *x*, 1 − *y*, −*z*; $ = 2 − *x*, 1 − *y*, −*z*.

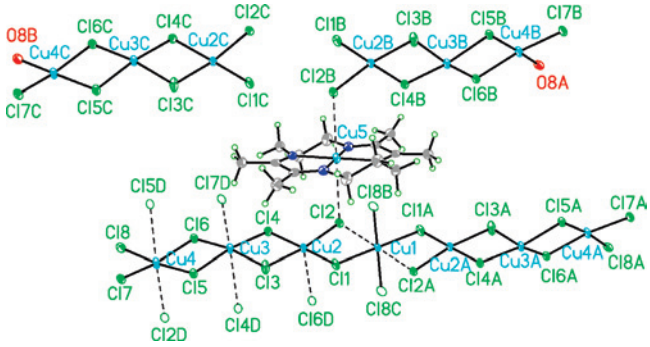

Figure 4. Illustration of the basic structural elements in $[Cu(TIM)]_2$-$Cu_{13}Cl_{30}(H_2O)_2 \cdot xH_2O$. Semicoordinate Cu···Cl bonds are shown as dashed lines. Semicoordinate bond lengths: Cu1−Cl2, 2.625; Cu5−Cl6D, 2.815; Cu3−Cl4, 3.202; Cu3−Cl7D, 2.612; Cu4−Cl2D, 2.818; Cu4−Cl4d, 3.063; Cu5−Cl2, 2.920 Å.

and yet each sheet remains surprisingly flat. A pair of water molecules lies above and below each perforation and are affixed to the sheet by means of two O−H···Cl contacts, as shown in Figure 3. The water molecules form strong hydrogen bonds to the chloride ions at the edges of the excisions, stabilizing the layer structure. Two *trans*-$[DBA]^+$ cations, (Figure 1) with the long axis of the molecule running roughly parallel to the [0 4 1] direction, connect the water molecules of adjacent sheets as shown. The orientation of each cation allows it to hydrogen bond to two water molecules of different layers via one N−H···O bond and one bifurcated hydrogen bond to create dimensional stability within the lattice.

$[Cu(TIM)]_2Cu_{13}Cl_{30}(H_2O)_2 \cdot xH_2O$. The structure of this triclinic salt is much more complicated than that of the Cd salt described above, both because of the Jahn−Teller distortion present for the Cu ions and because of a systematic disorder that is present in the structure. Figure 4 attempts to illustrate these two aspects of the structure. In the structure, the sites for Cu1, Cl8, and O8 are occupied 50% of the time. In addition, another site is partially occupied (∼14%) by a lattice−water molecule (not shown in Figure 4). The Cu1 site is located on a center of inversion. The symmetrically bibridged trimeric Cu_3Cl_7L unit (L = Cl^- or H_2O), containing Cu2, Cu3, and Cu4, constitutes the basic building block of the structure. Each copper ion has a basic square planar coordination geometry, with the Cu−Cl distances ranging from 2.243 to 2.358 Å. Cu3 and Cu4 complete a distorted 4 + 2 octahedral coordination through the formation of two semicoordinate bonds to chloride ions in adjacent trimeric units, while Cu2 assumes a 4 + 1 coordination.[20] The $Cu(TIM)^{2+}$ moieties bridge between two such trimeric units (from adjacent layers) via semicoordinate Cu···Cl bonds to Cl2 and Cl2B (Figure 4). A symmetry-related $Cu(TIM)^{2+}$ cation also forms a semicoordinate bond to Cl2A. Thus, both Cl2 and Cl2A are involved in Cu···Cl linkages to Cu5 atoms of the adjacent cations, forcing the reorientation of the Jahn−Teller elongation axis for Cu1. Within a layer, when the Cu1 site is occupied, adjacent trimeric units are linked to form heptameric $Cu_7Cl_{14}L_2$ units. When the Cu1 site is unoccupied, the adjacent Cl8 sites (Cl8B and Cl8C in Figure 4) are occupied by O8 water molecules.

Figures 5a and 5b illustrate the perforated layers found in this compound. Systematic excisions of $(Cu_2Cl_2)^{2+}$ fragments occur where the edges of the unit cell pass through the layers. This leads to the perforations shown in the figure. Random excisions of $CuCl_2$ species, with the concomitant insertion of pairs of water molecules, occur at the Cu1 site, as illustrated on the left-hand side of the figures. As seen in Figure 5b, this excision links adjacent sites of $(Cu_2Cl_2)^{2+}$ fragment excisions along the *a* axis. The water molecules form hydrogen bonds across the vacated Cu1 site, as shown by the dashed lines in Figure 5a. It should be noted that if these excisions/replacements were not random, a doubling of the unit cell would have had to occur.

(20) The sixth site is occupied 14% of the time by the lattice−water molecule.

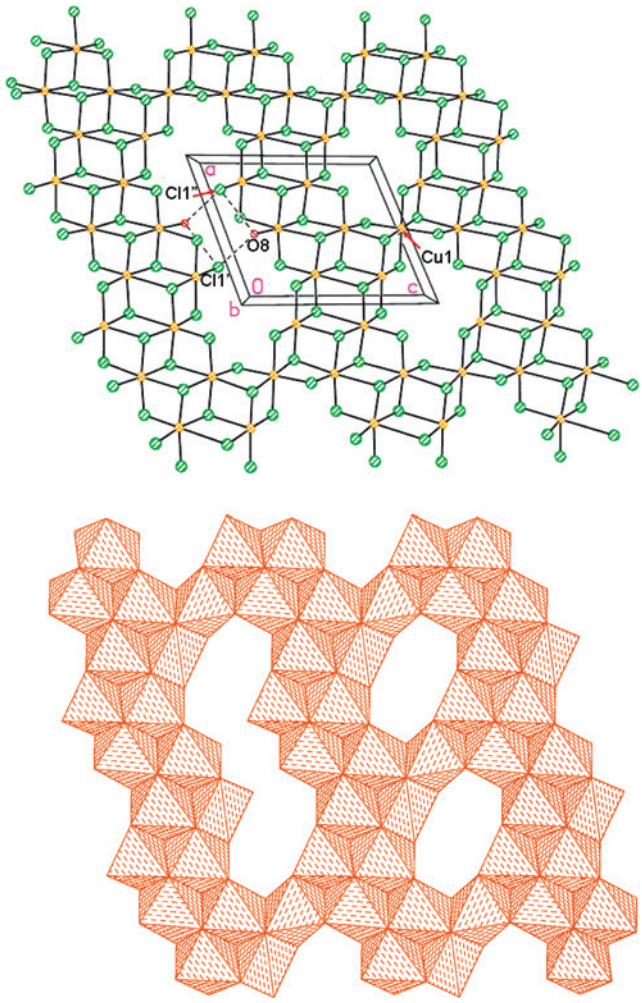

Figure 5. Ball and stick model (top) and polyhedral representation of the perforated layer in $[Cu(TIM)]_2Cu_{13}Cl_{30}(H_2O)_2 \cdot xH_2O$, lying athwart the $y = 1/2$ plane, illustrating the perforations formed by the removal of the $Cu_2Cl_2^{2-}$ fragments. The left-hand portion shows the configuration when the Cu1 site is unoccupied and water molecules replace Cl8 atoms associated with that site. The dashed lines denote O−H···Cl hydrogen bonds (O8−Cl1′ = 3.268, O8−Cl1″ = 3.134 Å).

Coverage of the layers by the $Cu(TIM)^{2+}$ cations is illustrated in Figure 6. A centrosymmetrically related set of cations lie on the opposite side of each layer. These cations are centered above (and below) the Cu1 sites, rather than over the sites of the $Cu_2Cl_2^{2-}$ excisions. This is in contrast to the Cd salt, where the water molecules cover the excision sites, as well as to the previously reported Cu salts, where the organic cations sit athwart the excision sites.

Discussion

These two structures demonstrate two new modes of interaction by which perforated layers can be generated from the parent layers of edge-shared octahedra. The Cd salt is unique in several ways. It is the first example where the layers were not based on the ferrodistortive $CuCl_2$ lattice[21] but on the undistorted hexagonal $CdCl_2$ type layers.[22] In addition, this is the first example where bare M^{2+} ions have been excised from the layers. This possibility of extracting

(21) Wells, A. F. *J. Chem. Soc.* **1947**, 1670.

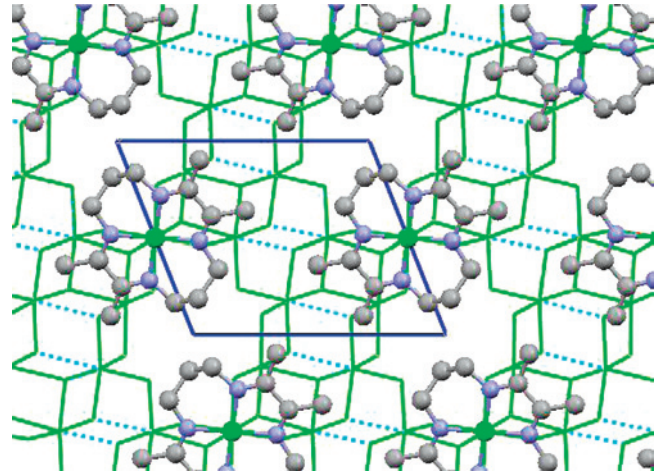

Figure 6. Illustration of the coverage of the perforated layers by the Cu(TIM) ions. A Cu5 copper atom of a $Cu(TIM)^{2+}$ cation sits directly above (and below) each Cu1 site.

simple metal ions is associated with the hydrogen bonding capabilities of the DBA^+ cations and the concomitant inclusion of the water molecules. The cations and water molecules are able to hydrogen bond to the chloride ions at the sites of the excisions and thereby stabilize the structure at these sites

The Cu structure presents the first example of the incorporation of a divalent cation into a perforated layer structure. The copper macrocycle system links the layers together via the formation of Cu···Cl semicoordinate bonds to chloride ions on adjacent layers, resulting in a displacement of the cations away from the centers of the incisions. Thus, the centers of positive and negative charges are offset. This leads to the disorder observed at the Cu1 site, where 50% of the $CuCl_2$ units at that site are removed to reduce the accumulation of positive electrostatic charge built up by the incorporation of the divalent cations.

We have previously argued that because it is not possible to pack more than two cations about each hole, the removal of fragments with more than a −2 charge would be energetically unfavorable.[13a] This argument was based on the presence of monovalent cations. With divalent cations, the excision of more highly negative charged fragments could theoretically be possible. However, in this case, the presence of the copper macrocyclic species allows for the formation of the semicoordinate bonds linking adjacent layers, thus retaining the +2 charge ratio per excision.

Acknowledgment. We thank Prof. Norman Rose, University of Washington, for providing this Cu(TIM) salt and NSF-EPSCoR and the M. J. Murdock Charitable Trust (UI) for support of the X-ray facility.

Supporting Information Available: Tables of data collection and refinement parameters, positional and thermal parameters, bond distances and angles, and CIF files. This material is available free of charge via the Internet at http://pubs.acs.org.

IC8000834

(22) Pauling, L.; Hoard, J. L. *Z. Kristallogr. Kristallgeom. Kristallphys. Kristallchem.* **1930**, *74*, 546.